A numerical investigation of turbulent forced convection through a TCC (trapezoidal) and SCC (Semicircle) corrugated tube

Mahendra Pratap Pal[1,*]
[1]Department of Mathematics, Jaypee Institute of Information Technology, Noida India, mpfatehpur@gmail.com
Lokendra Kumar[2]
[2]Department of mathematics, Jaypee Institute of Information technology Noida India, lokendma@gmail.com

Abstract

With Reynolds numbers ranging from 5,000 to 25,000 and a constant heat flux of 1x104 W m2, an experimental study is conducted to investigate the effects of turbulent nanofluid flow on thermo-hydraulic performance in corrugated channels. With a volume percentage of 1% to 5%, Al2O3 water nanofluids are used to build and test SCC ("semicircle corrugated channels") and TCC ("corrugated channels"). Using ANSYS Fluent, a numerical analysis of turbulent forced convection through a TCC (trapezoidal) and SCC (semicircle) corrugated tube is presented. According to the experimental results, using corrugated channels (TCC) enhances thermal performance by up to 2 times and heat transmission levels up to 63.59% when compared to SCC. Due to the rise in thermal conductivity, heat transport also increased when Al2O3 volume percentage rose. In comparison to using the same channels with base fluid, the heat transfer ratio increased by about 7.9–8.3% when the tested channels were utilised with Al2O3 nanofluid at 2.0% volume percentage. The tube being studied has a diameter of 8 mm, a length of 200 mm, and a uniform constant heat flux of 5,000 W/m2 delivered at the boundary with the corrugated wall.

Keywords— Heat convection, corrugated channel, TCC, SCC, Al2O3, nanofluid

DOI Number: 10.14704/nq.2022.20.15.NQ88128 **NeuroQuantology 2022; 20(15):1411-1422**

1. Introduction

Heat transfer is an important problem in thermal engineering and it has a big impact on our lives. One of the major issues in a wide range of industries is the ability to remove or add enough heat from one process stream to another. In addition to conduction, fluid is used to transfer energy in vehicles, freezers, heat exchangers, air conditioners, cooling systems etc. The primary phenomenon that regulates the behaviour of heat transport is fluid. Several techniques have been developed in the recent few decades to increase efficiency of heat transfer and decrease pumping power

etc. Some of these techniques include the use of the physical system's extended surface, the use of microchannels etc. Increasing the working fluid's thermal conductivity can also help with heat transfer through the channel. Most researchers are currently focusing more on increasing the thermal conductivity of working fluids. Heat transfer fluids are frequently utilised, and these include water, engine oil and ethylene glycol,. In contrast to the thermal conductivity of solids, fluid has low and thermal conductivity of the base or working fluid can be considerably improvedby including a tiny amount of solid particles. Thus, a number of researchers have already explored the use of solids particles of sizes 2 millimetres or micrometres [1,2,3]. Researchers use Al_2O_3, CuO, Ti_2O etc. nanoparticle frequently for preparing nanofluid [4,5]. Due to their excellent thermal conductivity and capacity for heat transmission, these nanoparticles are used. The performance and choice of nanoparticle are influenced by particle size and shape. Because of this, Eastman et al. [6] have concentrated primarily on the possible application of NFs in heat transfer.
The utilisation of Al_2O_3 (“alumina nanofluids”) to enhance the performance of corrugated channels with range of 5,000 to 25,000 Re was put to the test in an experimental comparison test.

2. Literature Review

Sheikholeslami et al. conducted a n experiment on how the form of nanoparticles affected the behaviour of nanofluids. Results demonstrated that nanoparticle shape can alter the thermal conductivity of the base fluid. The study further concluded that Nusselt number can also be a shape factor [7].

Mousavi et al. used a two-phase mixture model to study the hydrothermal properties of a nanofluid. The experiments used a water-Fe_3O_4 nanofluid as a coolant and the control volume approach. By combining a nanofluid flow in corrugated channels under the magnetic field, higher thermal performance was attained [8].

In order to assess PEC, Akbarzadeh et al. used wavy lenses and nanofluids. In their simulations, SST k-w models and multi-phase mixture were used. According to their findings, triangular walls provided a superior Nu number than sinusoidal walls. Furthermore, it was shown that employing nanofluid, which took into account the maximum thermal performance, boosted PEC for sinusoidal channels by 72% [9].

An analytical investigation through asymmetric wavy channels was conducted by Mosayebidorcheh et al. to examine the heat transfer and flow. It worked well with a variety of factors, including geometry, Brownian motion, Dufour, and Soret numbers. Brownian motion parameter increases have been demonstrated for its impact on heat transfer [10].

Using an alumina nanofluid, Toghraie et al. explored PEC in plate heat exchangers. The effects of nanoparticle concentration, flow rate, perforation diameter, and waviness aspect ratio were studied. According to their findings, corrugated/perforated fns were used to produce the greatest PEC of 1.95. Additionally, when compared to the base fluid, Al_2O_3 nanofluid reported the best rate of HTC [11].

Manca et al. performed a study for the range of 20,000 and 60,000 reynolds number using Al_2O_3 nanofluid and ribbed channel. In terms of nanofluids, single-phase tests were conducted on volume fractions of nanoparticle ranging from 0.0 to 0.04 with particle sizes of 38 nm. Their findings showed that when the Φ increased, heat transmission and Δp improved. Rectangular shapes have been determined to have the highest PEC when compared to square shapes [12].

In order to study how different nanoparticle forms affect the improvement of thermodynamic performance and heat transfer, Elias et al. performed an analytical methodology. A solution of water and ethylene glycol was used to scatter Al_2O_3 nanoparticles of various shapes. For higher heat transfer performance in the heat exchanger, nanoparticles of cylindrical-shape were ideal for improving performance [13].

3. Methodology

Data gathered from each test is represented by the wall and bulk fluid temperatures, flow rate, pressure drop, current, and voltage.

3.1 Principal equations

Continuity equation:

$$\frac{\partial}{\partial x_i}(\rho u_i) = 0$$

Momentum equation:

$$\frac{\partial}{\partial x_i}(-\rho u_i T) = \frac{\partial}{\partial x_j}\left((\Gamma + \Gamma_t)\frac{\partial T}{\partial x_j}\right)$$

Energy equation:

$$\frac{\partial(\rho u_i u_j)}{\partial x_j} = -\frac{\partial p}{\partial x_i} + \frac{\partial}{\partial x_j}\left[\mu\left(\frac{\partial u_i}{\partial x_j} + \frac{\partial u_j}{\partial x_i}\right)\right] + \frac{\partial}{\partial x_j}(-\rho \overline{u_i' u_j'})$$

Here, the expressions for turbulent thermal diffusivity Γ and molecule thermal diffusivity Γ_t are:

$$\Gamma = \frac{\mu}{Pr'}$$

$$\Gamma_t = \frac{\mu_t}{\mathrm{Pr}_t'}$$

According to the definition of eddy viscosity and the Boussinesq relationship, the normal Reynoldsstress is given by:

$$(-\rho \overline{u_i' u_j'}) = \mu_t\left(\frac{\partial u_i}{\partial x_j} + \frac{\partial u_j}{\partial x_i}\right)$$

The formula of turbulent eddy viscosity is:

$$\mu_t = \rho C_\mu \frac{k^2}{\varepsilon}$$

Turbulent kinetic energy

$$\frac{\partial}{\partial t}(\rho k) + \frac{\partial}{\partial x_j}(\rho k u_j) = \frac{\partial}{\partial x_j}\left[\left(\mu + \frac{\mu_t}{\sigma_k}\right)\frac{\partial k}{\partial x_j}\right] + G_k + G_b - \rho\varepsilon - Y_M + S_k$$

Turbulent dissipation rate

$$\frac{\partial}{\partial y}(\rho\varepsilon) + \frac{\partial}{\partial x_j}(\rho\varepsilon u_j) = \frac{\partial}{\partial x_j}\left[\left(\mu + \frac{\mu_t}{\sigma_\varepsilon}\right)\frac{\partial \varepsilon}{\partial x_j}\right] + \rho C_1 S\varepsilon - \rho C_2 \frac{\varepsilon^2}{k + \sqrt{v\varepsilon}} + C_{1\varepsilon}\frac{\varepsilon}{k}C_{3\varepsilon}G_b + S_\varepsilon$$

Where,

$$C_1 = \max\left[0.43, \frac{\eta}{\eta+5}\right],\ \eta = S\frac{k}{\varepsilon} \text{ and } S = \sqrt{2S_{ij}S_{ij}}$$

G_k = Generation of turbulent kinetic energy due to mean velocity gradients

G_b = Generation of turbulent kinetic energy due to buoyancy

σ_k = turbulent for k

σ_ε = turbulent for ε

Y_M= Fluctuating dilatation in compressible turbulence's contribution

3.2 Fluid dynamics and Thermal Properties

The following formula is used for calculating Reynolds number

$$\mathrm{Re} = \frac{\rho u_{\mathrm{in}} D_{\mathrm{h}}}{\mu}$$

The following equation can be used to determine the heat produced by fluid across the test section.$Q_f = \dot{m}_{nf}\, C_{p,nf}\, (Tb_{out} - Tb_{in})$

The definition of bulk temperatures T_b is given by

$$T_b = \frac{\int_0^R uTdA_c}{\int_0^r udA_c}$$

Where A_c = cross-sectional area of the circular section. The average heat transfer coefficient h_c is given by

A_w = surface area of the circular tube

$$h_c = \frac{Q_{nf}}{A_w\left(\Delta T_m\right)}$$

Δ T_m = Temperature difference between fluid and the wall and represented in the following equation

$$\Delta T_m = \left(T_w - T_t\right)$$

The expression of average Nusselt number is defined as follows 1414

$$Nu = \frac{h_c D_h}{K_{nf}}$$

The pumping power in turbulent flow is:

$$W = \frac{(\pi/4) D_h^{\,2} U_{av} \Delta P}{L}$$

Using eqn (1) the electric power is determined by measuring the current (I) and voltage (V)$Q_{heate}r$ = I × V

The hydraulic diameter (D_h) and friction factor (f) can be defined as

$$D_{\mathrm{h}} = \frac{4A_{\mathrm{C}}}{P}$$

$$f = \Delta p \frac{D_{\mathrm{h}}2}{L_{\mathrm{corr}} \rho_{\mathrm{nf}} u_{\mathrm{in}}^2}$$

Dynamic viscosity for selected nanofluid is

$$\mu_{nf} = \mu_f(1+7.3\phi+123\phi^2)$$

Thermal conductivity for selected nanofluid is

$$k_{nf} = k_{bf}\left(1.0021+7.3349\phi\right)$$

It is possible to compute the density of the nanofluid as well as the particle volume concentrationand individual attributes.

$$\rho_{nf} = \rho_{bf}\left(1-\phi\right)+\rho_p\phi$$

Utilizing the particle volume concentration and individual parameters, the specific heat capacityof the nanofluid may be calculated.

$$C_{nf} = C_{bf}\left(1-\phi\right)+C_p\phi$$

3.3 Code Validation

In the current study, numerical evaluations of heat transfer behaviour and pumping power needsthrough a TCC and SCC tube have been conducted using ANSYS Fluent software. Figure 1 demonstrates the association that Notter and Sleicher made, The correlation developed by Notter and Sleicher is as follows:

$$N_u = 5 + 0.016\, Re^a\, Pr^b$$

Where

$$a = 0.88 - \frac{0.24}{4+\Pr} \text{ and } b = 0.33 + 0.5e^{-0.6\Pr}$$

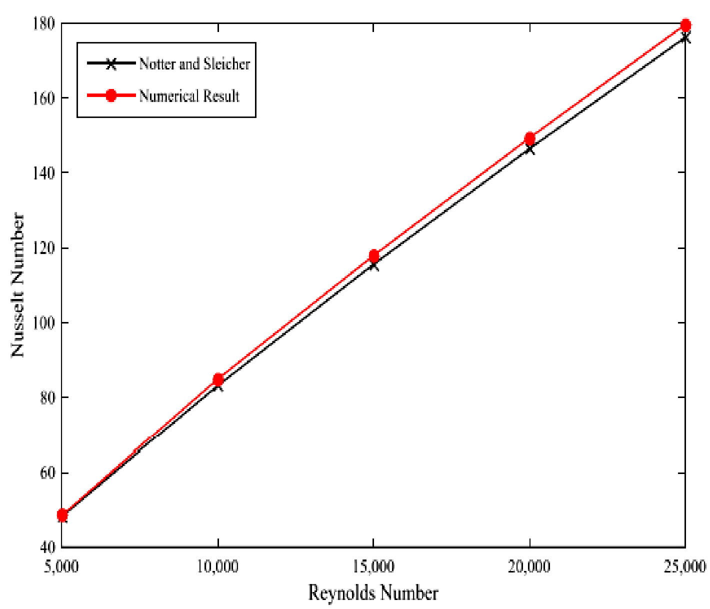

Figure 1 Illustration of Nusselt number comparison between Sleicher and Notter

3.4 Grid Independence Test

The simulation was ran at Re = 5,000 withAl_2O_3 as the working substance for the grid independence research. To determine the ideal grid size for the current investigation, a grid independence test was conducted.

Table 1 Characteristics of tested channels

Description	Character	TCC Value	SCC Value
Height of channel	*H*	10	10
Width of channel	*W*	50	50
Height of corrugation	*h*	2.5	2.5
Corrugation width	*w*	5	5
Longitudinal pitch	*p*	15	15
Corrugation small height	*e*	1	–

Figure 2 Front view of (a) SCC, (b) TCC

Table 2 Thermophysical Properties of Al_2O_3 – Water Nanofluid

Property	1%	2%	3%	4%	5%
Density (ρ)	1026.3241	1056.0582	1085.7923	1115.5264	1145.2605
Thermal Conductivity (κ)	0.6562	0.7010	0.7458	0.7905	0.8353
Specific Heat (C_p)	4145.158	4111.116	4077.074	4043.032	4008.99
Viscosity (μ)	0.000968	0.001066	0.001186	0.001328	0.001492

4. Results

This section analyses and describes the effects of Al_2O_3-water nanofuids on heat transmission, PEC and pressure drop across the TCC and SCC.

4.1 Nusselt Number

Figure 3 depicts the relationship between the Nusselt number for Al2O3-water and the volume fraction and Re. From the figure the Nusselt number of each nanofluid employed in the current study rises as the Re and volume percentage of the nanofluids rise. This happened as a result of anincrease in effective thermal conductivity, a rise in energy exchange rate, and the erratic, chaotic motion of ultrafine particles in nanofluids brought on by volume fraction and increase in Re. In general, larger fluid velocity and temperature gradient are correlated with higher Reynolds numbers, which in turn leads to higher Nusselt numbers.

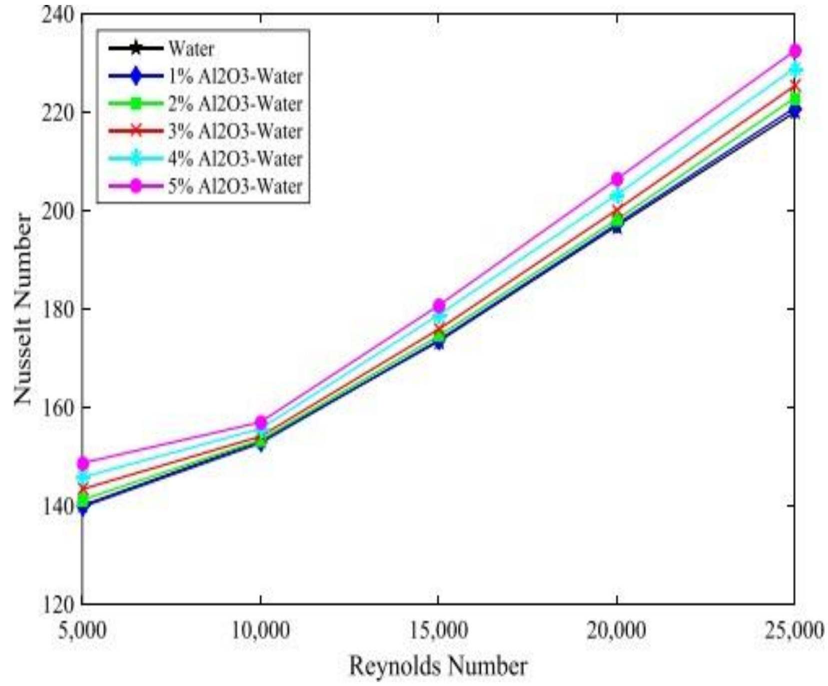

Figure 3 Illustration of Nusselt Number for Al_2O_3 at 1% to 5% volume

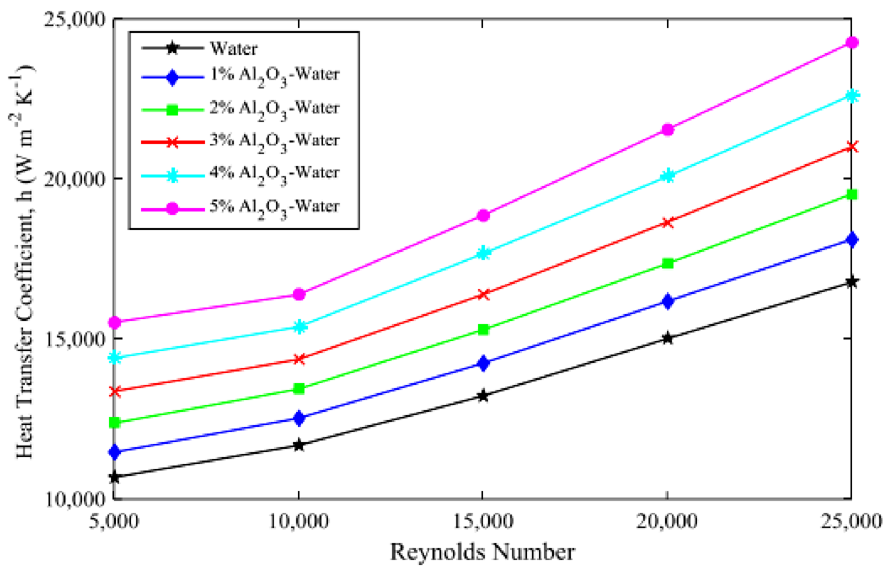

Figure 4 Illustartion of Heat Transfer Coefficient for Al_2O_3 at 1% to 5% volume

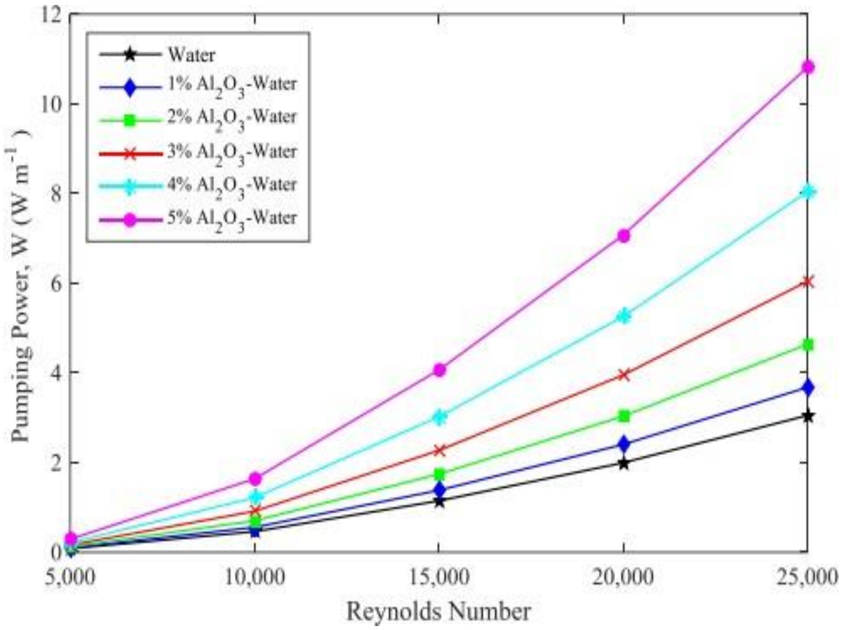

Figure 5 Illustration of power of Al_2O_3 at 1% to 5% volume

5. Discussion

5.1 Heat transfer rate and Impact of corrugated channels

In this part, Al2O3-water has been used to examine the effects of channels on the outcomes of theNu and p tests as well as the SC tests. Nu can be significantly improve and Improving Re translates to increasing coolant mass flow rate. Both the (TCC) and (SCC) channels examined resulted in higher Nu. The actual reasons in this instance are the generation of secondary flows and flow development, and flow intensity is primarily determined by the geometric model and secondarily by the characteristics of the coolant. The impact in this instance is because the discoveries in this section are focused on the same fluid.

5.2 Impact of Al_2O_3–water nanofluid

The Nu_{av} rises with an increase in Re number for each of the channels examined in the current study, as would be predicted. Contrary to the basic coolant, increasing Re has a significant effect on Nu_{av}. In fact, raising Re has been observed to produce chaotic movements of nanoparticles than decreasing Re. When the rises, the Nu_{av} rises at a specific Re. The nanopowder to enhance the thermal conductivity of the base fluid is explained. The results also revealed that TCC is superiorto SCC in both volume fractions, indicating the importance of the corrugation form in enhancing heat transfer.

5.3 Impact of Heat loss and Pressure drop

By measuring the Δp for the flow related to the friction loss across the tested channels, the hydraulic performance may be evaluated. The usage of corrugated channels increased the Δp morethan that of Straight Channels. Besides an increase in contact surface area, the blending factor alsocaused the Δp to increase as Re increased.

6. Conclusions

To observe how varied nanofluid volume fractions affect heat transfer coefficient and pumping power, the following conclusions are drawn. Using ANSYS Fluent tool, the heat transfer of nanofluid Al_2O_3 in TCC and SCC has been examined. Both the Re number and the volume percentage of nanofluid contribute to an increase in the heat transfer coefficient. With Re ranging from 5,000 to 25,000 and a constant heat flux of $1x10^4$ W m^2, a numerical study is conducted to investigate the effects of different corrugated walls and turbulent nanofluid flow. With a volume percentage of 1% to 5%, Al_2O_3 water nanofluids are used to build and test semicircle corrugated channels and trapezoidal corrugated channels (TCC).

References

1. Salami M, Khoshvaght-Aliabadi M, Feizabadi A. Investigation of corrugated channel performance with diferent wave shapes. J Therm Anal Calorim. 2019;138(5):3159–74.

2. Ajeel RK, Salim WI, Hasnan K. Thermal performance comparison of various corrugated channels using nanofluid: numerical study. Alex Eng J. 2019;58(1):75–87.

3. Abdelrazek AH, Kazi SN, Alawi OA, Yusof N, Oon CS, Ali HM. Heat transfer and pressure drop investigation through pipe with diferent shapes using diferent types of nanofuids. J Therm Anal Calorim. 2020;139(3):1637–53.

4. Khan A, Ali HM, Nazir R, Ali R, Munir A, Ahmad B, Ahmad Z. Experimental investigation ofenhanced heat transfer of a car radiator using ZnO nanoparticles in H2O–ethylene glycol mixture. J Therm Anal Calorim. 2019;138(5):3007–21.

5. Abdulwahab MR. A numerical investigation of turbulent magnetic nanofluid fow inside square straight channel. J Adv Res Fluid Mech Therm Sci. 2014;1(1):44–52.

6. Heidary H, Hosseini R, Pirmohammadi M, Kermani MJ. Numerical study of magnetic feld efecton nano-fuid forced convection in a channel. J Magn Magn Mater. 2015;374:11–7.

7. Sahar AM, Wissink J, Mahmoud MM, Karayiannis TG, Ishak MS. Efect of hydraulic diameter and aspect ratio on single phase fow and heat transfer in a rectangular microchannel. Appl Therm Eng. 2017;115:793–814.

8. Hussein AM, Dawood HK, Bakara RA, Kadirgamaa K. Numerical study on turbulent forced convective heat transfer using nanofuids TiO2 in an automotive cooling system. Case Stud Therm Eng. 2017;9:72–8.

9. Delavari V, Hashemabadi SH. CFD simulation of heat transfer enhancement of Al2O3/water and Al2O3/ethylene glycol nanofuids in a car radiator. Appl Therm Eng. 2014;73(1):380–90.

10. Shahsavani E, Afrand M, Kalbasi R. Using experimental data to estimate the heat transfer and pressure drop of non-Newtonian nanofluid fow through a circular tube: applicable for use in heat exchangers. Appl Therm Eng. 2018;129:1573–81.

11. Ho CJ, Lee CY, Yamada M. Experiments on laminar cooling characteristics of a phase change nanofluid fow through an iso-flux heated circular tube. Int J Heat Mass Transf. 2018;118:1307– 15.

12. Sheikholeslami M, Jafaryar M, Li Z. Nanofluid turbulent convective flow in a circular duct with helical turbulators considering CuO nanoparticles. Int J Heat Mass Transf. 2018;124:980–9.

13. Behroyan I, Ganesan P, He S, Sivasankaran S. Turbulent forced convection of Cu–water nanofluid: CFD model comparison. Int Commun Heat Mass Transf. 2015;67:163–72.

14. Kumar N, Puranik BP. Numerical study of convective heat transfer with nanofluids in turbulent flow using a Lagrangian–Eulerian approach. Appl Therm Eng. 2017;111:1674–81.

15. Mills ZG, Warey A, Alexeev A. Heat transfer enhancement and thermal–hydraulic performance in laminar flows through asymmetric wavy walled channels. Int J Heat Mass Transf.2016;97:450–60.

16. Pati S, Mehta SK, Borah A. Numerical investigation of thermohydraulic transport characteristics in wavy channels: comparison between raccoon and serpentine channels. Int Commun Heat Mass Transf. 2017;88:171–6.

17. Ramgadia AG, Saha AK. Numerical study of fully developed unsteady fow and heat transfer in asymmetric wavy channels. Int J Heat Mass Transf. 2016;102:98–112.

18. Akbarzadeh M, Rashidi S, Esfahani JA. Infuences of corrugation profles on entropy generation, heat transfer, pressure drop, and performance in a wavy channel. Appl Therm Eng. 2017;116:278–91.

19. Baik YJ, Jeon S, Kim B, Jeon D, Byon C. Heat transfer performance of wavy-channeled PCHEs and the efects of waviness factors. Int J Heat Mass Transf. 2017;114:809–15.

20. Arman S, Hassanzadeh R. Effects of the geometric parameters on the thermal-hydraulic performance of the wavy tubes. Int Commun Heat Mass Transf. 2018;96:27–36.

21. Harikrishnan S, Tiwari S. Effect of skewness on flow and heat transfer characteristics of a wavy channel. Int J Heat Mass Transf. 2018;120:956–69.

22. Akbarzadeh M, Maghrebi MJ. Combined efects of corrugated walls and porous inserts on performance improvement in a heat exchanger channel. Int J Therm Sci. 2018;127:266–76.

23. Esmaeili M, Sadeghy K, Moghaddami M. Heat transfer enhancement of wavy channels using Al2O3 nanoparticles. J Enhanc Heat Transf. 2010;17(2):139–51.

24. Ajeel RK, Salim WI, Hasnan K. Impacts

of corrugation profles on the fow and heat transfer characteristics in trapezoidal corrugated channel using nanofuids. J Adv Res Fluid Mech Therm Sci. 2018;49(2):170–9.

25. Ajeel RK, Salim WI, Hasnan K. Thermal and hydraulic characteristics of turbulent nanofuids fow in trapezoidal-corrugated channel: symmetry and zigzag shaped. Case Stud Therm Eng. 2018;12:620–35.

26. Ajeel RK, Salim WI, Hasnan K. Thermal performances comparison in various types of trapezoidal corrugated channel using nanofuids. Int Rev Mech Eng. 2018;12(8):672–83.

27. Ajeel RK, Salim WS, Hasnan K. Numerical investigations of flow and heat transfer enhancement in a semicircle zigzag corrugated channel using nanofuids. Int J Heat Technol. 2018;36(4):1292–303.